Supporting Information for:

CQDs doped magnetic electrospun nanofibers: Fluorescence self-display and adsorption removal of mercury (II)

Lei Li,[†,‡] Feijun Wang,[†,‡] Yanyan Lv,[†,‡] Jianxin Liu,[†,‡] Hongli Bian,[†,‡] Wenjun Wang,[†,‡] Yonghong Li,[†] and Ziqiang Shao,[†,‡]*

† School of Materials Science and Engineering, Beijing Institute of Technology, Beijing 100081, China

‡ Beijing Engineering Research Centre of Cellulose and Its Derivatives, Beijing 100081, China

KEYWORDS. Carbon quantum dots, fluorescence monitoring, mercury removal, magnetic Fe_3O_4, chitosan, electrospinning nanofibers

* To whom correspondence should be addressed.

E-mail: wangfj@bit.edu.cn

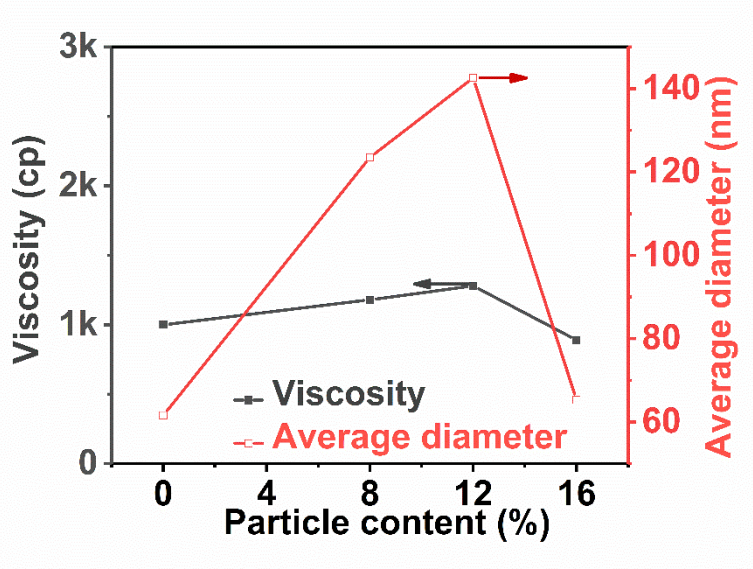

Figure S1. Relationship of the viscosity of the spinning solution and average diameters of nanofibers.

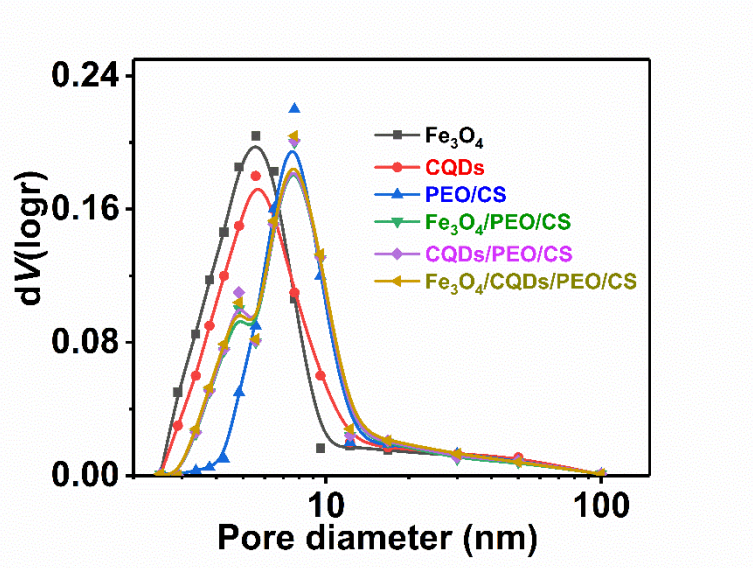

Figure S2. Pore-size distribution of different samples.

Table S1. Textural characteristics of the samples

Samples	Specific surface area S_{BET}/(m^2 g^{-1})	Pore volume /(cm^3 g^{-1})	Average pore diameter *D*/nm
Fe_3O_4	78.675	0.238	3.231
CQDs	79.249	0.303	3.104
PEO/CS	32.281	0.102	14.381
Fe_3O_4/PEO/CS	34.123	0.113	10.542
CQDs/PEO/CS	36.565	0.126	13.129
Fe_3O_4/CQDs/PEO/CS	38.234	0.141	11.632

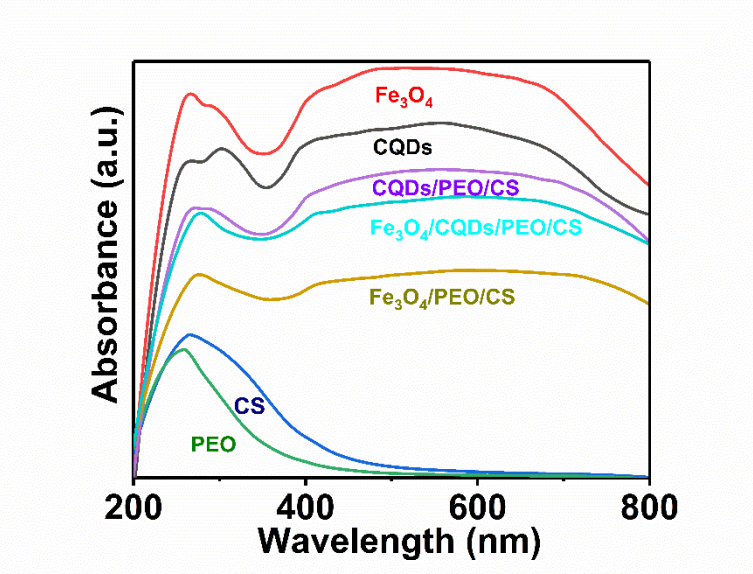

Figure S3. UV-vis diffuse reflectance spectroscopy of different samples.

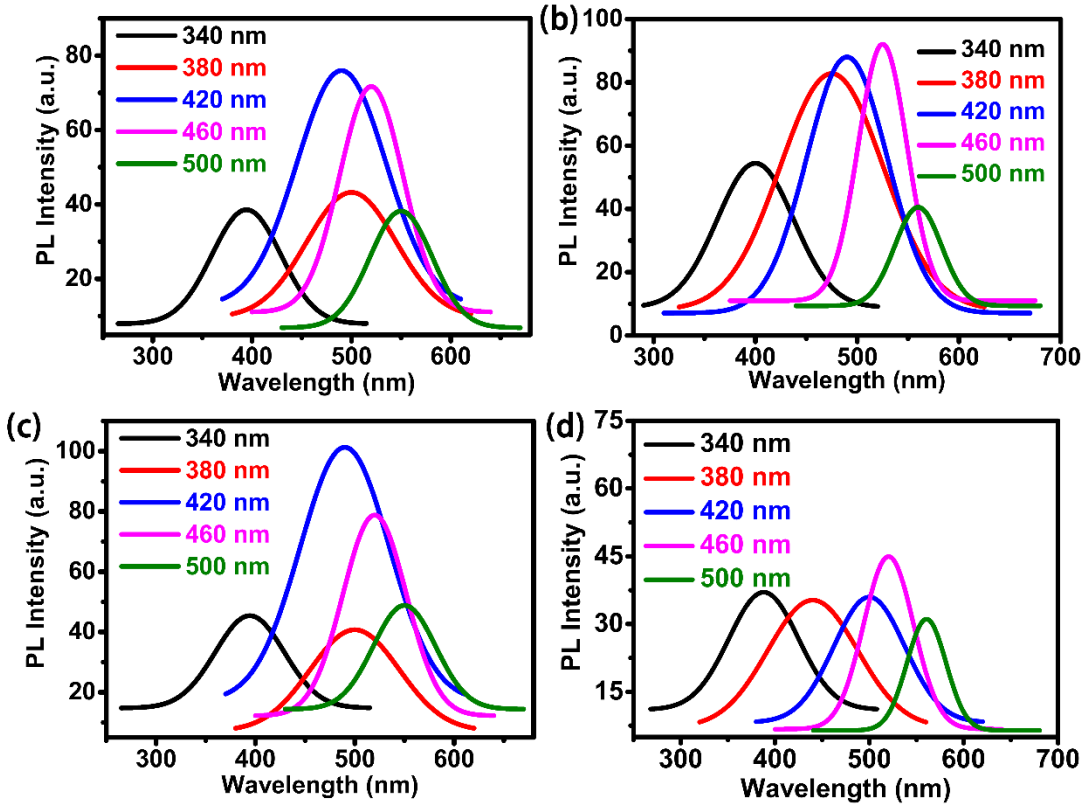

Figure S4. PL spectra of CQDs/PEO/CS with CQDs contents of 4% (a), 5% (b), 6% (c), and 7% (d).

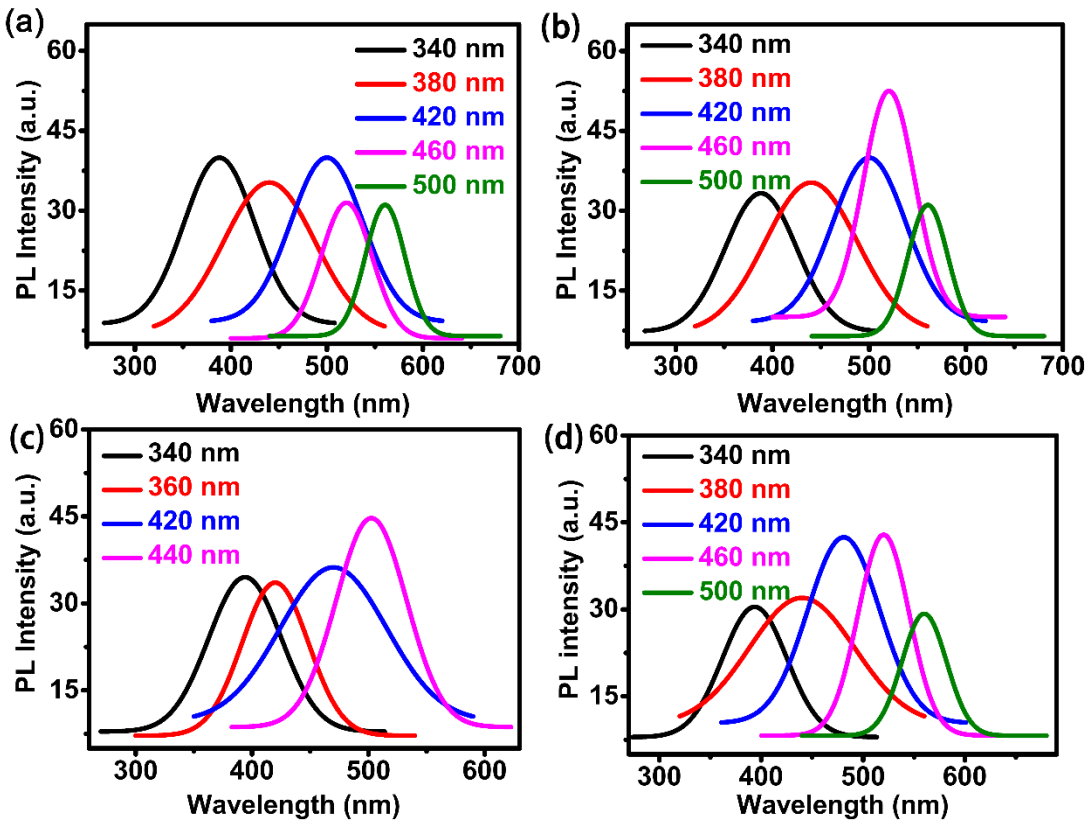

Figure S5. PL spectra of Fe_3O_4/CQDs/PEO/CS with nanoparticle contents of 8% (a), 10% (b), 12% (c), and 14% (d). In each of the nanofibers, the content of Fe_3O_4 and CQDs is equal.

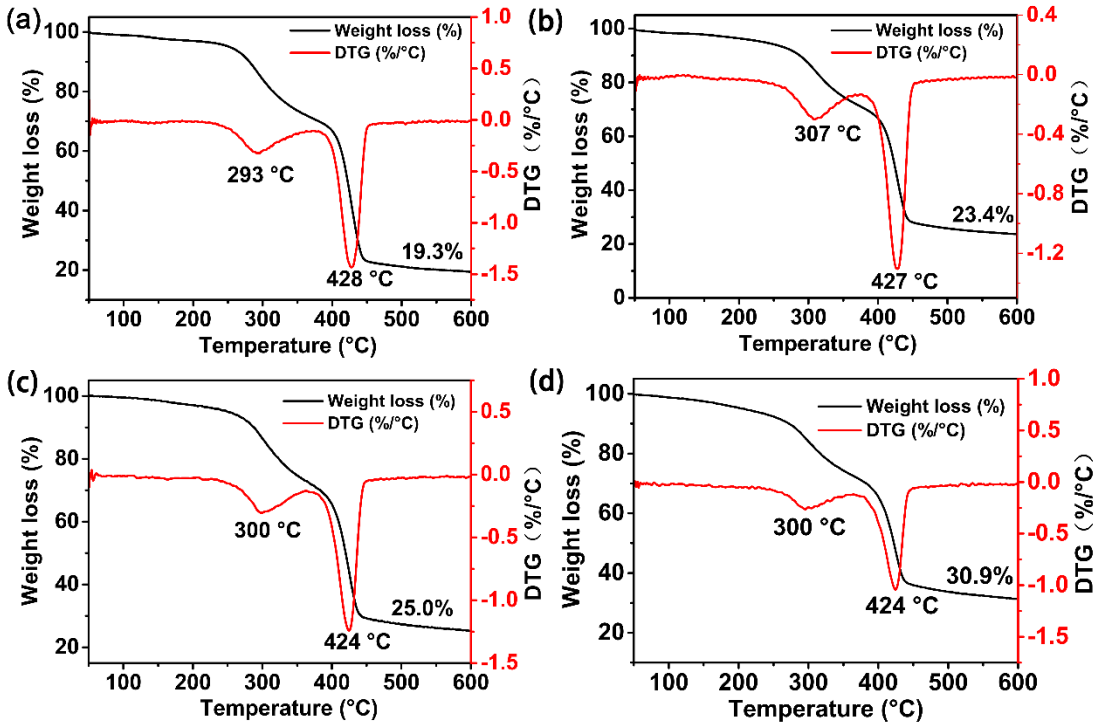

Figure S6. TG and DTG curves of electrospun nanofiber membranes with different content. (a)

Pristine PEO/CS nanofibers, (b) 4% Fe_3O_4 and 4% CQDs, (c) 6% Fe_3O_4 and 6% CQDs, and (d) 8% Fe_3O_4 and 8% CQDs.

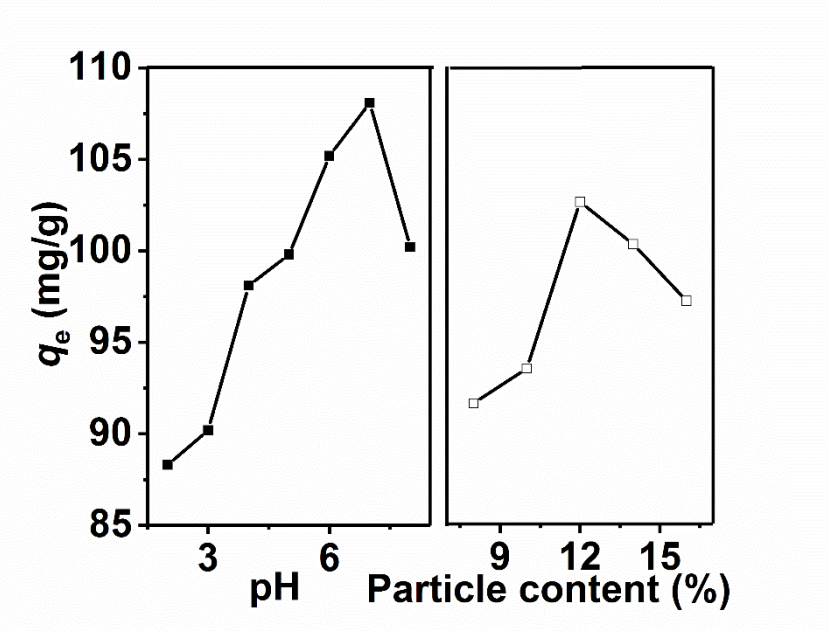

Figure S7. Effect of pH values and particle contents on equilibrium adsorption capacity.

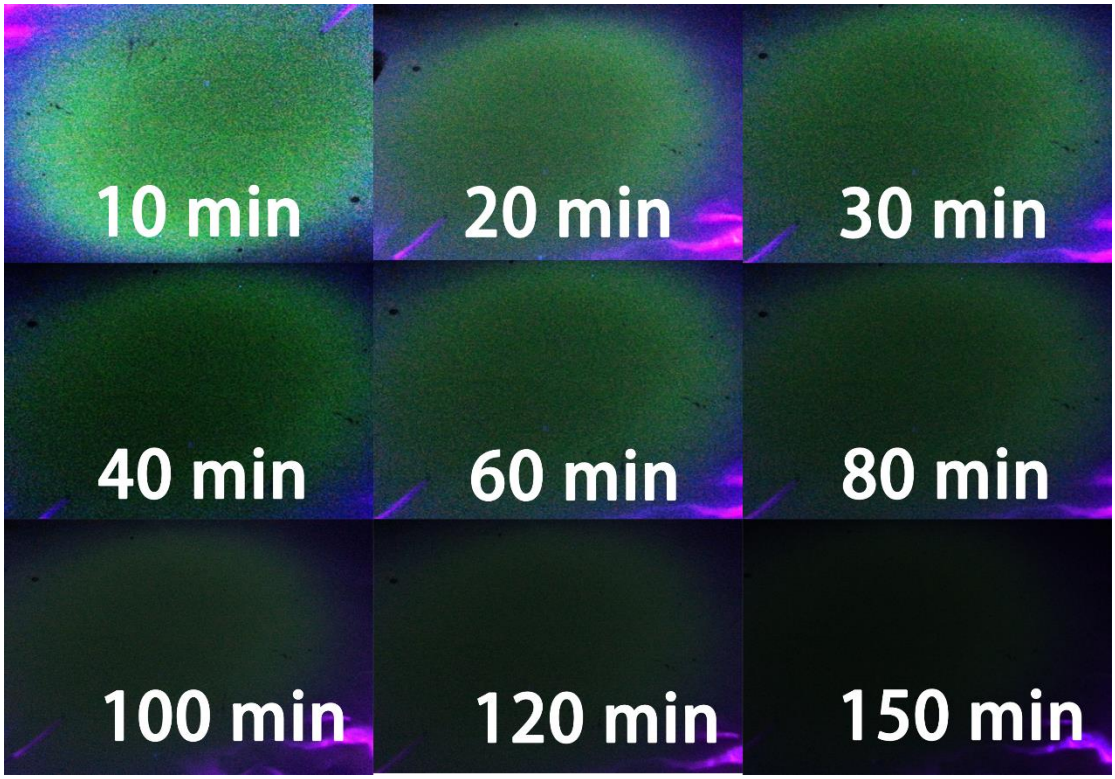

Figure S8. The photos of Membrane 1 under UV excitation (420 nm) at different adsorption time.

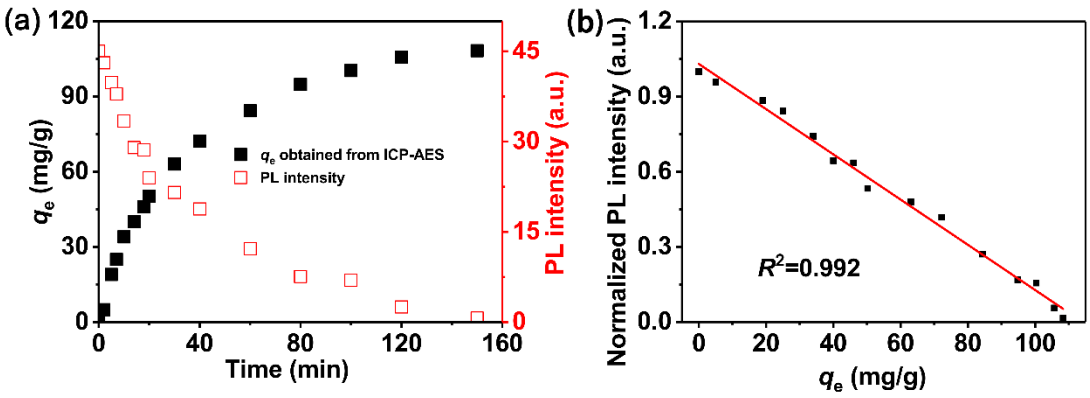

Figure S9. (a) Comparison of fluorescence detection and ICP-AES results in real rainwater samples. (b) The liner fitting result of normalized PL intensity versus accumulative adsorption capacity in real rainwater samples.

Table S2. Kinetic parameters of Hg(II) ions adsorption onto the Fe_3O_4/CQDs/PEO/CS nanofibrous adsorbent.

Pseudo-first-order model			Pseudo-second-order model			Intraparticle diffusion model		
q_e (mg/g)	k_1 (min^{-1})	R^2	q_e (mg/g)	k_2 (g/mg min)	R^2	k_i (mg/g min)	C (mg/g)	R^2
105.636	-0.0278	0.982	131.061	0.000246	0.999	9.702	2.661	0.970

Table S3. Isotherm parameters and thermodynamic parameters for Hg(II) sorption onto the Fe_3O_4/CQDs/PEO/CS nanofibrous adsorbent

T (°C)	Langmuir isotherm			Freundlich isotherm			ΔH (kJ/mol)	ΔS (kJ/mol K)	ΔG (kJ/mol)
	q_m (mg/g)	k_L (L/mg)	R^2	k_F (mg/g)	n	R^2			
25	148.148	0.0214	0.997	9.642	1.985	0.958	6.511	0.0302	-2.493
35	149.701	0.0221	0.996	10.689	2.062	0.966			-2.795
45	151.515	0.0229	0.994	11.662	2.127	0.970			-3.097